Temperature and configurational effects on the Young's modulus of poly (methyl methacrylate)

Sahputra, Iwan Halim; Alexiadis, Alessio; Adams, Michael

DOI:
10.1080/08927022.2018.1450983

Document Version
Peer reviewed version

Citation for published version (Harvard):
Sahputra, IH, Alexiadis, A & Adams, M 2018, 'Temperature and configurational effects on the Young's modulus of poly (methyl methacrylate): a molecular dynamics study comparing the DREIDING, AMBER and OPLS force fields', *Molecular Simulation*, vol. 44, no. 9, pp. 774-780. https://doi.org/10.1080/08927022.2018.1450983

Temperature and configurational effects on the Young's modulus of poly (methyl methacrylate): a molecular dynamics study comparing the DREIDING, AMBER and OPLS force fields

Iwan H. Sahputra, Alessio Alexiadis, Michael J. Adams

School of Chemical Engineering, University of Birmingham, Birmingham, United Kingdom

Corresponding author: Iwan H. Sahputra, I.H.Sahputra@bham.ac.uk

Abstract The effects of the configuration and temperature on the Young's modulus of poly (methyl methacrylate) (PMMA) have been studied using molecular dynamics simulations. For the DREIDING force field under ambient temperatures, increasing the number of monomers significantly increases the modulus of isotactic and syndiotactic PMMA while the isotactic form has a greater modulus. The effects of temperature on the modulus of isotactic PMMA have been simulated using the DREIDING, AMBER, and OPLS force fields. All these force fields predict the effects of temperature on the modulus from 200 to 350 K that are in close agreement with experimental values, while at higher temperatures the moduli are greater than those measured. The glass transition temperature determined by the force fields, based on the variation of the modulus with temperature, is greater than the experimental values, but when obtained from a plot of the volume as a function of the temperature, there is closer agreement. The Young's moduli calculated in this study are in closer agreement to the experimental data than those reported by previous simulations. .

Keywords: Poly (methyl methacrylate) (PMMA), DREIDING, AMBER, OPLS, Young's modulus

1. Introduction

Poly (methyl methacrylate), PMMA, is classified as a polyacrylate and is biocompatible and non-biodegradable. Consequently, it can be used alone as a matrix material or as a minor phase to improve some properties of biodegradable matrices [1]. In addition to its mechanical stability and strength, low cost and ease of manufacture, it has some properties that make it a valuable material for biomedical and pharmaceutical applications, such as non-toxicity and minimal inflammatory reactions with tissues [2]. Examples of biomedical applications include microspheres [1, 3], microcapsules [4, 5], dental [6, 7], implants [8, 9], bone cements [10, 11], and contact lenses [12, 13].

For such applications, it is crucial to fully understand the impact of the raw material properties on the final products. Hlinak et al. [14] presented a set of critical material properties in pharmaceutical formulations and for process developments of solid dosage

forms. For example, the elastic modulus of microsphere materials will influence the final mechanical properties of the dosage form. This is also the case for other polymeric materials, e.g. the degree of polymerization and molecular weight of microcrystalline cellulose show a strong positive impact on tablet strength [15, 16]. Therefore it is important to be able to measure material properties by laboratory experiments or to predict them by mathematical modelling. Such modelling has an advantage compared to an experimental approach since it can provide a more fundamental scientific understanding of the parameters governing the properties.

Molecular dynamics (MD) simulation has been increasingly employed to predict the mechanical properties of polymers. It is based on an empirical mathematical model of the potential energy of atoms and classical equations of motion in order to simulate the interactions and dynamics of materials at an atomistic level. However, to derive more reliable predictions of the macroscopic properties of polymers, a large number of conditions needs to be studied and compared to laboratory data. For PMMA, some MD simulations have been performed to study its various properties, however there are discrepancies between the results and experimental values.

Jaramillo et al. [17] developed a PMMA model consisting of 1080 chains, where each has 96 monomers, to study how volumetric and deviatoric strains influence the yield behaviour for a wide range of loading conditions. They observed that permanent deformation occurred when either the deviatoric or volumetric strains reached critical values. Kim et al. [18] developed two models based on five and also forty 96-monomer chains in order to characterise the molecular structure, thermal properties and energetics of PMMA films. The calculated free surface energies agreed closely with experimental measurements and they observed that the annealing process had a strong effect on the molecular structure. Sane et al. [19] constructed a model of amorphous PMMA consisting of 3 chains, where each chain had

50 monomers, and calculated the bulk compliance as a function of temperature. Near room temperature, their results were consistent with experimental values, however, the variation of the compliance with temperature could not be reproduced completely.

Soldera and Grohens [20] performed MD simulations of PMMA chains with different tacticity to investigate the glass transition behaviour and carried out energetic and local dynamics analyses. Their simulated glass transition temperature (Tg) for isotactic PMMA (i-PMMA) and syndiotactic PMMA (s-PMMA) are higher than experimental values, however, the difference in the two values is in close agreement with experimental data. Mohammadi et al. [21] attempted to estimate the Tg of i-PMMA by employing the united atom model consisting of 3 chains each with 100 monomers. To achieve this objective, the polymer properties including the thermal conductivity, volume, thermal expansion and Young's modulus were examined. They found that the Young's modulus ranged from 1.9 – 1.2 GPa in the temperature range of 300 – 600 K. The values at low temperatures up to room temperature were less than experimental values while at high temperatures they were higher, and the simulated Tg was higher than experimental values.

The aim of the current study is to present a further exploration of MD simulations that reproduce the effects of tacticity, number of monomers per chain (degree of polymerisation) and temperature on the elastic properties of PMMA. The previous work did not include these factors, for example, they did not consider the effects of different numbers of monomers on the properties and the numbers of monomers were much fewer than commercial PMMA. The mechanical properties of PMMA, such as the toughness, improve with increasing molecular weight up to a limiting value of ~ 10^5, which corresponds about 1000 monomer units [22]. Therefore, it is necessary to build PMMA models with more monomer units since the previous simulations were unable to produce results that were in close agreements with

experiments, e.g. in terms of the smaller Young's modulus at room temperature or higher Tg values.

The suitability of three force fields is also evaluated for reproducing the effects of temperature on the Young's modulus of i-PMMA. In MD simulations, the force field used to describe the interaction between atoms and molecules is one of the most important factors influencing the accuracy of the simulated system and its properties. The force fields evaluated and compared for the first time in this study are the DREIDING [23], AMBER [24], and OPLS all-atom [25]. These force fields were selected because they have been employed in previous studies of PMMA. The DREIDING force field has been validated by comparing i-PMMA crystals to X-ray structural analysis data [19] and has been applied to study the Tg of s-PMMA [26]. The AMBER force field has been used to study syndiotactic and isotactic oligomers of PMMA and is able to reproduce quantitatively the experimental X-ray scattering results obtained in dilute solutions of benzene, especially for syndiotactic oligomers ofPMMA [27]. The OPLS force field has been validated by direct comparison to structural and dynamic neutron scattering measurements, and by comparison via temperature extrapolation of activation energies and rotational times for methyl group rotations [28]. It also has been used to study the effects of tactility and temperature on the surface structure of PMMA at a polymer−vacuum interface [29].

2. Modelling and simulation

The initial structures of PMMA, -[CH_2-$C(CH_3)(OCOCH_3)$]- , were created using Polymer Modeler [30]. To study the various configurations, six models were created (Table 1), where each model has 5 chains. Figure 1 shows the structure of a single chain i-PMMA and s-PMMA models containing 4 monomers visualised using Jmol [31]. The ester groups of i-PMMA are projected on the same side of the polymer chain while for the syndiotactic form,

they are projected in a regular alternation on both sides of the polymer chain. The tacticity of polymers influences their physical properties such as the Tg and solubility. The parameters for DREIDING, AMBER and OPLS force fields were those reported in references [19], [27], and [28] respectively.

The Polak-Ribiere version of the conjugate gradient algorithm [32] was employed to minimise the energy of the initial structure, with a force stopping criteria of 10^{-9}. The MD simulations were then performed under isothermal conditions for 50 ps at two high temperatures (600 and 1000 K) with the temperature controlled by a Langevin thermostat. Two different initial temperatures were selected in order to study the effects of the annealing temperature on the mechanical properties. Subsequently, further simulations of 50 ps duration were conducted under isobaric-isothermal conditions at the same temperature and zero pressure, where the temperature and pressure were controlled using a Nose-Hoover barostat and thermostat respectively. The temperature was cooled to the required value (200, 250, 300, 350, 400, 450, 500, 550, 600, 650, and 700 K) within 100 ps again using a Nose-Hoover barostat and thermostat. The model was then subjected to seven equilibration process cycles with each cycle composed of an energy minimization using the conjugate gradient algorithm and an equilibration process for 50 ps under isobaric-isothermal conditions at the specified temperature and zero pressure. The measurement of the volume of the samples corresponded to a duration of 50 ps after equilibration.

To compute the Young's moduli, MD simulations of uniaxial extension were implemented using LAMMPS [33] with periodic boundary conditions. Each model was stretched sequentially in orthogonal directions to a true strain of 2% at a constant strain rate of 10^9 s^{-1}. The stretching duration was 21 ps. The mean values of the Young's moduli were calculated from the gradients of the stress-strain curves.

3. Result and discussion

Table 2 presents the Young's modulus for the two PMMA configurations calculated from the simulations using the DREIDING force field at 300 K. For comparison, experimental values at strain rates of 4 x 10^{-5} and 4 x 10^{-2} s^{-1} are 3.4 and 6.3 GPa respectively [34]. Information about the tacticity of the sample was not available, however, commercial PMMA materials generally have 50-70% syndiotactic, about 30% atactic, and <10% isotactic [35] configurations.

To the authors' knowledge, data have not been published for the Young's modulus of both pure i- PMMA and s-PMMA. However, increasing the chain regularity and isotacticity of polypropylene has been shown to be accompanied by proportionally greater increase in the stiffness [36]. Moreover, the barrier energy of the ester methyl groups for rotation in i-PMMA is greater than in s-PMMA [37] [38], which implies higher local order and stronger non-bonded interactions with neighbouring groups. The current simulations show that the dihedral angle energy for i-PMMA is greater than for s-PMMA e.g. for 400 monomer models, the energy is 4182 and 3763 kcal/mole for i-PMMA and s-PMMA respectively. Therefore, it is expected that i-PMMA has a greater stiffness than s-PMMA, which is consistent with the simulated data shown in Table 2.

It can be seen in table 2 that the Young's moduli of the samples containing 400 monomers are greater than the published experimental data in [34] measured at the lowest strain rate, but smaller than the one measured at the fastest strain rate. It is well known that the Young's modulus of a polymer increases with increasing strain rate [34]. The simulations involved a much higher strain rate than the highest experimental value, however, the moduli are lower. This can be explained by the differences between the simulations and experiment, in term of number of monomers and thermal history, as discussed below.

In [34] information is not given about the number of monomers, however, commercial PMMA materials may consist of about 1300 – 22,000 monomers [39]. While the largest model considered here has only 400 monomers, which is relatively small compared to commercial PMMA, but is a higher molecular weight than considered previously in published models (100 monomers or less). The smaller molecular weight of the models contributes to the lower Young's modulus compared to the experimental values. It has been shown that the molecular weight of PMMA influences the flexural modulus of cross-linked dentures based on this polymer [7]; increasing the molecular weight from 120,000 to 220,000 (corresponding to an increase in the number of monomers from about 1,200 and 2,200 respectively) significantly increases the modulus. The molecular weight of PMMA also influences the modulus at room temperature measured using the dynamic mechanical analysis technique (DMA) [40] and the modulus of elasticity measured using transverse deflection [41]. The current work also shows a similar trend of an increase in the Young's modulus with an increase of the number of monomer units (Table 2). It may be concluded that the DREIDING force field is satisfactorily in this respect.

The mechanical behaviour of glassy polymers is known to be dependent on their thermal history, such as quenching and annealing. Annealed samples of polycarbonate, poly(vinyl chloride), polystyrene, and poly(methyl methacrylate) have been shown to have a greater yield stress and Young's modulus than the quenched samples [42-44]. Quenched polymer samples have a greater enthalpy change measured by differential scanning calorimetry, which is consistent with the greater degree of structural disorder preserved by quenching [43]. By quenching, the mobility of polymer molecules is reduced therefore they cannot organize themselves periodically to form a crystal structure, hence the relatively smaller yield stress and modulus. The fast cooling rate for preparing the samples in the MD

simulations also contributes to the calculated Young's modulus being smaller than the experimental values.

Table 3 presents the influence of the annealing temperature on the Young's modulus of i-PMMA and s-PMMA calculated at various temperature using the DREIDING force field. There is not a significant discrepancy between the values calculated from the two annealing temperatures; the difference between them is within the statistical deviation of the calculation. However, at a temperature of 500 K, the model annealed at 1000 K tends to give a smaller Young's modulus, which is closer to experimental values. It should be emphasised that the selection of the current annealing temperatures (600 and 1000 K) did not significantly influence the Young's modulus of the polymers calculated at ambient temperatures. However, for investigating the effect of temperature, the annealing temperature was set at 1000 K since the results were in closer agreement with experimental data at high temperatures.

The effect of temperature on the Young's modulus calculated using the three force fields is presented in Figure 2. For this purpose, an i-PMMA model with 400 monomers/chain and an annealing temperature of 1000 K was used. As would be expected, the figure shows that increasing the temperature reduces the Young's modulus. A similar trend has been found for the storage modulus of PMMA measured by DMA, for example [45] and [46].

At room temperature, the Young's modulus is about 3.74, 3.69 and 4.68 GPa for the simulations using the DREIDING, AMBER, and OPLS force fields respectively; the measured storage modulus at 1 Hz is about 3 [46] and 5 GPa [45]. The storage modulus is approximately equal to the elastic modulus for a single, rapid stress at low strain in the linear viscoelastic region [47]. Therefore under ambient temperatures, the three force fields are able to reproduce the Young's modulus in close agreement with the experimental data. At

temperatures between 200 - 300 K, all force fields also predicted that the Young's modulus is in close agreement with experimental data, which are between 4.8 – 3 GPa [46] and 7.3 – 5 GPa [45], where the OPLS predicted a greater modulus than the other two force fields.

It can be observed in Figure 2 that for all force fields there is a sharp decrease (about 1 GPa) in the Young's modulus for the temperature range of 450 to 500 K. This indicates a transition between the glassy and rubbery regions of PMMA. In [45] and [46], such reductions (about 2.1 and 1.3 GPa respectively) were measured between 380 and 400 K corresponding to the Tg (381 and 388 K respectively). These Tg values indicate that the samples are composed mainly of syndiotactic configurations.

According to [48], the measured Tg of s-PMMA is between 328 and 397 K depending on the degree of polymerisation, while for i-PMMA it is between 295 and 323 K, and also depends on the degree of polymerisation. The current values for i-PMMA are higher than the measured Tg. It is known that the Tg determined by thermomechanical techniques depends on the deformation rate. Therefore, the origin of the discrepancy could be the much higher strain rate applied in the MD simulations compared to those applied in the DMA. The higher strain rate in the current simulations results in a shorter time for the polymer chains to reorientate when stretched, and hence the Tg is higher.

At high temperatures (> 350 K), the current simulations using all force fields cannot reproduce the measured values of the Young's modulus although the OPLS predicted greater modulus values than the other two force fields. For example, at 400 K the measured values of the Young's modulus are about 0.1 [46] and 0.03 GPa [45]. It is possible that the greater values computed here arise from the much greater imposed strain rates, which restricts the mobility of the chains under uniaxial tension. For the DREIDING potential, Sane et al [19] reported that the bulk compliance of PMMA at high temperatures (> 350 K) also cannot be reproduced accurately compared to experimental values.

When a polymer is stretched, the chains-ends are moved apart and the conformations are changed. The methyl side groups (CH_3 and $OCOCH_3$) of PMMA hinders the free rotation about the main C-C bonds, which is required to change the conformation. For example, in neutron scattering experiments, the ester methyl group is assumed to be in one of three states, with a dihedral angle of C-O-C-H approximately equal to 0 and $\pm 120^o$ and that the observed motion involves jumps between these states [49]. Thermal energy is required to activate such jumps in order to overcome the dihedral torsional energy, where at low temperatures the available thermal energies are insufficient. The temperature at which this jump can occur is related to the Tg. The computed changes in the dihedral torsional energy of i-PMMA as a function of temperature are presented in Figure 3. At about 350K, there is a small change in the gradient of the change in dihedral energy. This temperature corresponds to the computed Tg of i-PMMA. This is less than the value (450 to 500 K) determined from the Young's modulus – temperature curve (Figure 2). However, it is more consistent with the measured range of 295 – 323 K [48].

The cooling rate to prepare the sample in the MD simulations is much faster than the experimental rates, which contributes to the higher Tg. It is well known that cooling rate affects the Tg viz., increasing cooling rate increases Tg [50]. It has been shown for poly(vinyl acetate) that a ~5000 times faster cooling rate increased the Tg by about 8 K [51]. The effect of the cooling rate effect on the Tg also has been studied by MD simulations using a coarse-grained polymer model [52]; increasing the cooling rate by three orders of magnitude increased the Tg by about 9%. By cooling polymer melts very fast (i.e. quenching it) to far below the melting temperature, the mobility of the polymer molecules is immobilised to the extent that they cannot undergo translational or rotational motion in order to rearrange themselves periodically since there is insufficient vibrational energy. Thus, there is a correlation between increasing cooling rates and an increase in the Tg.

The Tg also corresponds to the change in the gradient in a dilatometrical plot of the volume as a function of the temperature. Figure 4 shows such a plot based on the current computed data, where the Tg is about 350 K, which is consistent with the value obtained in Figure 3. Again, this is higher than the measured range of 295 -323 K [48], possibly because of the higher cooling rates applied in the simulations, however it is more realistic than the previously published results of 430 K [20, 21] using other force field and the united atom model. The technique applied here to further equilibrate the model after cooling from a high annealing temperature, as described in the previous section, has reduced the effect of high cooling rates on the Tg hence the it is in closer agreement with the experimental values. A comparison between the experimental and simulated values of the Tg can be seen in Table 4.

The Tg has been considered to be related to the sudden change of expansion in the free volume of a polymer, for example as discussed in [53]. In Figure 3, it can be seen that at temperatures greater than the Tg of the current PMMA model, the change in the dihedral energy is greater than at temperatures less than the Tg. The thermal energy at high temperatures is sufficient for PMMA molecules to vibrate and overcome the energy barrier to rotation required for jumping to a different state. This mechanism increases the free volume, creating more space availabe for the polymer to undergo rotation and translation, and eventually reducing the Young's modulus above the Tg.

4. Conclusion

The effects of the number of monomers and tacticity on the Young's modulus of PMMA at ambient temperatures can be satisfactorily simulated using the DREIDING force field. Increasing the number of monomer units increases the Young's modulus of both isotactic and syndiotactic PMMA, which also has been observed experimentally. The calculated Young's modulus of isotactic PMMA is greater than the value for the syndiotactic form. In general,

the DREIDING, AMBER and OPLS force fields have similar performances in predicting the effects of temperature on the Young's modulus and Tg of isotactic PMMA. The effects of temperature on the Young's modulus from low temperatures to ambient values calculated using all force fields showed a similar trend to those measured. At ambient temperatures, all force fields reproduced the Young's modulus in close agreement with experimental values. However, for all force fields, because of much greater strain rates of the simulations compared to experiments, the computed Tg is higher and the Young's moduli predicted at temperatures above the Tg are greater. In contrast, the Tg predicted by all force fields from volume-temperature curves, is in closer agreement with experimental values. For the modulus at temperatures above the Tg, the OPLS force field is less accurate than the other two force fields.

Acknowledgements

This work was supported by the Engineering and Physical Sciences Research Council under Grant EP/M02959X/1. Molecular Dynamics simulations have been performed on the supercomputing system of the Institute of Process Engineering, Chinese Academy of Sciences.

References

1. Yuksel, N., et al., Investigation of triacetin effect on indomethacin release from poly(methyl methacrylate) microspheres: Evaluation of interactions using FT-IR and NMR spectroscopies. International Journal of Pharmaceutics, 2011. **404**(1): p. 102-109.
2. Ali, U., K.J.B.A. Karim, and N.A. Buang, *A Review of the Properties and Applications of Poly (Methyl Methacrylate) (PMMA).* Polymer Reviews, 2015. **55**(4): p. 678-705.
3. Bux, J., et al., *Manufacture of poly(methyl methacrylate) microspheres using membrane emulsification.* Philosophical Transactions of the Royal Society A: Mathematical, Physical and Engineering Sciences, 2016. **374**(2072).

4. Pan, X., et al., *Structure and Mechanical Properties of Consumer-Friendly PMMA Microcapsules.* Industrial & Engineering Chemistry Research, 2013. **52**(33): p. 11253-11265.
5. Kim, J.-W., et al., *Microencapsulation of cholesteryl alkanoate by polymerization-induced phase separation and its association with drugs.* Journal of Polymer Science Part A: Polymer Chemistry, 2004. **42**(9): p. 2202-2213.
6. Zuber, M., et al., *Biocompatibility and microscopic evaluation of polyurethane–poly(methyl methacrylate)–titanium dioxide based composites for dental applications.* Journal of Applied Polymer Science, 2014. **131**(3): p. n/a-n/a.
7. Kawaguchi, T., et al., *Influence of molecular weight of polymethyl(methacrylate) beads on the properties and structure of cross-linked denture base polymer.* Journal of the Mechanical Behavior of Biomedical Materials, 2011. **4**(8): p. 1846-1851.
8. Freitag, C.P.F., et al., *Endoscopic implantation of polymethylmethacrylate augments the gastroesophageal antireflux barrier: a short-term study in a porcine model.* Surgical Endoscopy, 2009. **23**(6): p. 1272-1278.
9. Itokawa, H., et al., *A 12 month in vivo study on the response of bone to a hydroxyapatite–polymethylmethacrylate cranioplasty composite.* Biomaterials, 2007. **28**(33): p. 4922-4927.
10. Nien, Y.-H., S.-w. Lin, and Y.-N. Hsu, *Preparation and characterization of acrylic bone cement with high drug release.* Materials Science and Engineering: C, 2013. **33**(2): p. 974-978.
11. Sugino, A., et al., *Relationship between apatite-forming ability and mechanical properties of bioactive PMMA-based bone cement modified with calcium salts and alkoxysilane.* Journal of Materials Science: Materials in Medicine, 2008. **19**(3): p. 1399-1405.
12. MacRae, S.M., M. Matsuda, and D.S. Phillips, *The Long-term Effects of Polymethylmethacrylate Contact Lens Wear on the Corneal Endothelium.* Ophthalmology. **101**(2): p. 365-370.
13. Hosaka, S., et al., *Mechanical properties of the soft contact lens of poly(methyl methacrylate-N-vinylpyrrolidone).* Journal of Biomedical Materials Research, 1980. **14**(5): p. 557-566.
14. Hlinak, A.J., et al., *Understanding critical material properties for solid dosage form design.* Journal of Pharmaceutical Innovation, 2006. **1**(1): p. 12-17.

15. Liao, Z., et al., *Multivariate analysis approach for correlations between material properties and tablet tensile strength of microcrystalline cellulose.* Die Pharmazie - An International Journal of Pharmaceutical Sciences, 2012. **67**(9): p. 774-780.
16. Shlieout, G., K. Arnold, and G. Müller, *Powder and mechanical properties of microcrystalline cellulose with different degrees of polymerization.* AAPS PharmSciTech, 2002. **3**(2): p. 45-54.
17. Jaramillo, E., et al., *Energy-based yield criterion for PMMA from large-scale molecular dynamics simulations.* Physical Review B, 2012. **85**(2): p. 024114.
18. Kim, Y.-j., K.-H. Lin, and A. Strachan, *Molecular dynamics simulations of PMMA slabs: role of annealing conditions.* Modelling and Simulation in Materials Science and Engineering, 2013. **21**(6): p. 065010.
19. Sane, S.B., et al., *Molecular dynamics simulations to compute the bulk response of amorphous PMMA.* Journal of Computer-Aided Materials Design, 2001. **8**(2): p. 87-106.
20. Soldera, A. and Y. Grohens, *Molecular modeling of the glass transition of stereoregular PMMAs.* Polymer-Plastics Technology and Engineering, 2002. **41**(3): p. 561-571.
21. Mohammadi, M. and J. Davoodi, *The glass transition temperature of PMMA: A molecular dynamics study and comparison of various determination methods.* European Polymer Journal, 2017. **91**: p. 121-133.
22. Beech, D.R., *Molecular weight distribution of denture base acrylic.* Journal of Dentistry, 1975. **3**(1): p. 19-24.
23. Mayo, S.L., B.D. Olafson, and W.A. Goddard, *DREIDING: a generic force field for molecular simulations.* The Journal of Physical Chemistry, 1990. **94**(26): p. 8897-8909.
24. Cornell, W.D., et al., *A Second Generation Force Field for the Simulation of Proteins, Nucleic Acids, and Organic Molecules.* Journal of the American Chemical Society, 1995. **117**(19): p. 5179-5197.
25. Jorgensen, W.L., D.S. Maxwell, and J. Tirado-Rives, *Development and Testing of the OPLS All-Atom Force Field on Conformational Energetics and Properties of Organic Liquids.* Journal of the American Chemical Society, 1996. **118**(45): p. 11225-11236.
26. Tsige, M. and P.L. Taylor, *Simulation study of the glass transition temperature in poly(methyl methacrylate).* Physical Review E, 2002. **65**(2): p. 021805.

27. Apel, U., R. Hentschke, and J. Helfrich, *Molecular dynamics simulation of syndio-and isotactic poly (methyl methacrylate) in benzene.* Macromolecules, 1995. **28**(6): p. 1778-1785.
28. Chen, C., J.K. Maranas, and V. García-Sakai, *Local Dynamics of Syndiotactic Poly(methyl methacrylate) Using Molecular Dynamics Simulation.* Macromolecules, 2006. **39**(26): p. 9630-9640.
29. Jha, K.C., et al., *Molecular Structure of Poly(methyl methacrylate) Surface II: Effect of Stereoregularity Examined through All-Atom Molecular Dynamics.* Langmuir, 2014. **30**(43): p. 12775-12785.
30. Haley, B.P., et al., *Polymer Modeler*. 2017.
31. *Jmol: an open-source Java viewer for chemical structures in 3D*.
32. Polak, E., Ribiere, G, *Note sur la convergence de méthodes de directions conjuguées.* ESAIM: Mathematical Modelling and Numerical Analysis - Modélisation Mathématique et Analyse Numérique, 1969. **3**(R1): p. 35-43.
33. Plimpton, S., *Fast Parallel Algorithms for Short-Range Molecular Dynamics.* Journal of Computational Physics, 1995. **117**(1): p. 1-19.
34. Li, Z. and J. Lambros, *Strain rate effects on the thermomechanical behavior of polymers.* International Journal of Solids and Structures, 2001. **38**(20): p. 3549-3562.
35. *Polymeric Materials Encyclopedia*, ed. J.C. Salamone. 1996: CRC Press.
36. Menyhárd, A.S., P.; László, Zs; Fekete, H. M.; Mester, O.; Horváth, Zs; Vörös, Gy; Varga, J.; Móczó, J., *Direct correlation between modulus and the crystalline structure in isotactic polypropylene.* Express Polymer Letters, 2015. **9**(3): p. 12.
37. Cereghetti, P.M., R. Kind, and J.S. Higgins, *Tacticity effects on the barriers to rotation of the ester methyl group in poly (methyl methacrylate): A deuteron magnetic resonance study.* The Journal of Chemical Physics, 2004. **121**(16): p. 8068-8078.
38. Gabrys, B., et al., *Rotational motion of the ester methyl group in stereoregular poly(methyl methacrylate): a neutron scattering study.* Macromolecules, 1984. **17**(4): p. 560-566.
39. Wypych, G., *Handbook of Polymers*. 2016: ChemTec Publishing.
40. Kusy, R.P. and A.R. Greenberg, *Influence of molecular weight on the dynamic mechanical properties of poly(methyl methacrylate).* Journal of thermal analysis, 1980. **18**(1): p. 117-126.

41. Huggett, R., J.F. Bates, and D.E. Packham, *The effect of the curing cycle upon the molecular weight and properties of denture base materials.* Dental Materials, 1987. **3**(3): p. 107-112.
42. Cross, A., R.N. Haward, and N.J. Mills, Post yield phenomena in tensile tests on poly(vinyl chloride). Polymer, 1979. 20(3): p. 288-294.
43. Hasan, O.A. and M.C. Boyce, Energy storage during inelastic deformation of glassy polymers. Polymer, 1993. 34(24): p. 5085-5092.
44. van Melick, H.G.H., L.E. Govaert, and H.E.H. Meijer, Localisation phenomena in glassy polymers: influence of thermal and mechanical history. Polymer, 2003. 44(12): p. 3579-3591.
45. Richeton, J., et al., *A unified model for stiffness modulus of amorphous polymers across transition temperatures and strain rates.* Polymer, 2005. **46**(19): p. 8194-8201.
46. Mulliken, A.D. and M.C. Boyce, *Mechanics of the rate-dependent elastic–plastic deformation of glassy polymers from low to high strain rates.* International Journal of Solids and Structures, 2006. **43**(5): p. 1331-1356.
47. *ISO 6721,* in *Plastics — Determination of dynamic mechanical properties-Part 1: General principles*. 2011.
48. Ute, K., N. Miyatake, and K. Hatada, *Glass transition temperature and melting temperature of uniform isotactic and syndiotactic poly(methyl methacrylate)s from 13mer to 50mer.* Polymer, 1995. **36**(7): p. 1415-1419.
49. Nicholson, T.M. and G.R. Davies, *Modeling of Methyl Group Rotations in PMMA.* Macromolecules, 1997. **30**(18): p. 5501-5505.
50. Moynihan, C.T., et al., *Dependence of the glass transition temperature on heating and cooling rate.* The Journal of Physical Chemistry, 1974. **78**(26): p. 2673-2677.
51. Kovacs, A.J., *La contraction isotherme du volume des polymères amorphes.* Journal of Polymer Science, 1958. **30**(121): p. 131-147.
52. Buchholz, J., et al., Cooling rate dependence of the glass transition temperature of polymer melts: Molecular dynamics study. The Journal of Chemical Physics, 2002. 117(15): p. 7364-7372.
53. White, R.P. and J.E.G. Lipson, *Polymer Free Volume and Its Connection to the Glass Transition.* Macromolecules, 2016. **49**(11): p. 3987-4007.

Table 1. PMMA models for the simulations

No	Configuration	Number of monomers in each chain	Total number of atoms
1	Isotactic PMMA (i-PMMA)	100	7510
2	Isotactic PMMA (i-PMMA)	200	15010
3	Isotactic PMMA (i-PMMA)	400	30010
4	Syndiotactic PMMA (s-PMMA)	100	7510
5	Syndiotactic PMMA (s-PMMA)	200	15010
6	Syndiotactic PMMA (s-PMMA)	400	30010

Table 2. Effect of configuration on the mean values Young's modulus calculated in three orthogonal directions at 300 K using the DREIDING force field

Number of monomer	**Young's modulus (GPa)**	
	s-PMMA	**i-PMMA**
100	2.82 ± 0.56	3.12 ± 0.68
200	2.74 ± 0.25	3.69 ± 0.60
400	3.60 ± 0.67	3.95 ± 0.47

Table 3. Effect of annealing temperature on Young's modulus at various temperature using the DREIDING force field.

Temperature (K)	**Young's modulus (GPa)**	
	Annealing temperature = 600 K	**Annealing temperature = 1000 K**
200	4.53 ± 0.55	4.14 ± 0.16
300	3.95 ± 0.47	3.74 ± 0.38
400	2.89 ± 0.23	3.10 ± 0.44
500	1.70 ± 0.24	1.52 ± 0.14

Table 4. Glass transition temperature of PMMA from experimental measurements and MD simulations

Method	**Glass transition temperature (K)**
Experiment s-PMMA[48]	328-397
Experiment i-PMMA[48]	295-323
MD simulations i-PMMA (modulus vs temperature)	450-500
MD simulations i-PMMA (volume vs temperature)	350

Figure 1. Structure of small (a) i-PMMA and (b) s-PMMA models. Red: oxygen, grey: carbon, white: hydrogen.

Figure 2. Effects of temperature on the Young's modulus for i-PMMA simulated using the AMBER, DREIDING and OPLS force fields. There is a sharp decrease in the Young's modulus between 450 and 500 K. Experimental values at ambient temperature are shown for comparison.

Figure 3. Change in the dihedral energy as a function of temperature for i-PMMA calculated using the AMBER, DREIDING and OPLS force fields. There is a small change in the gradient of the change in dihedral energy at about 350 K.

Figure 4. Volume as a function of temperature for i-PMMA calculated using the AMBER, DREIDING and OPLS force fields. There is a small change in gradient of the volume at about 350 K.

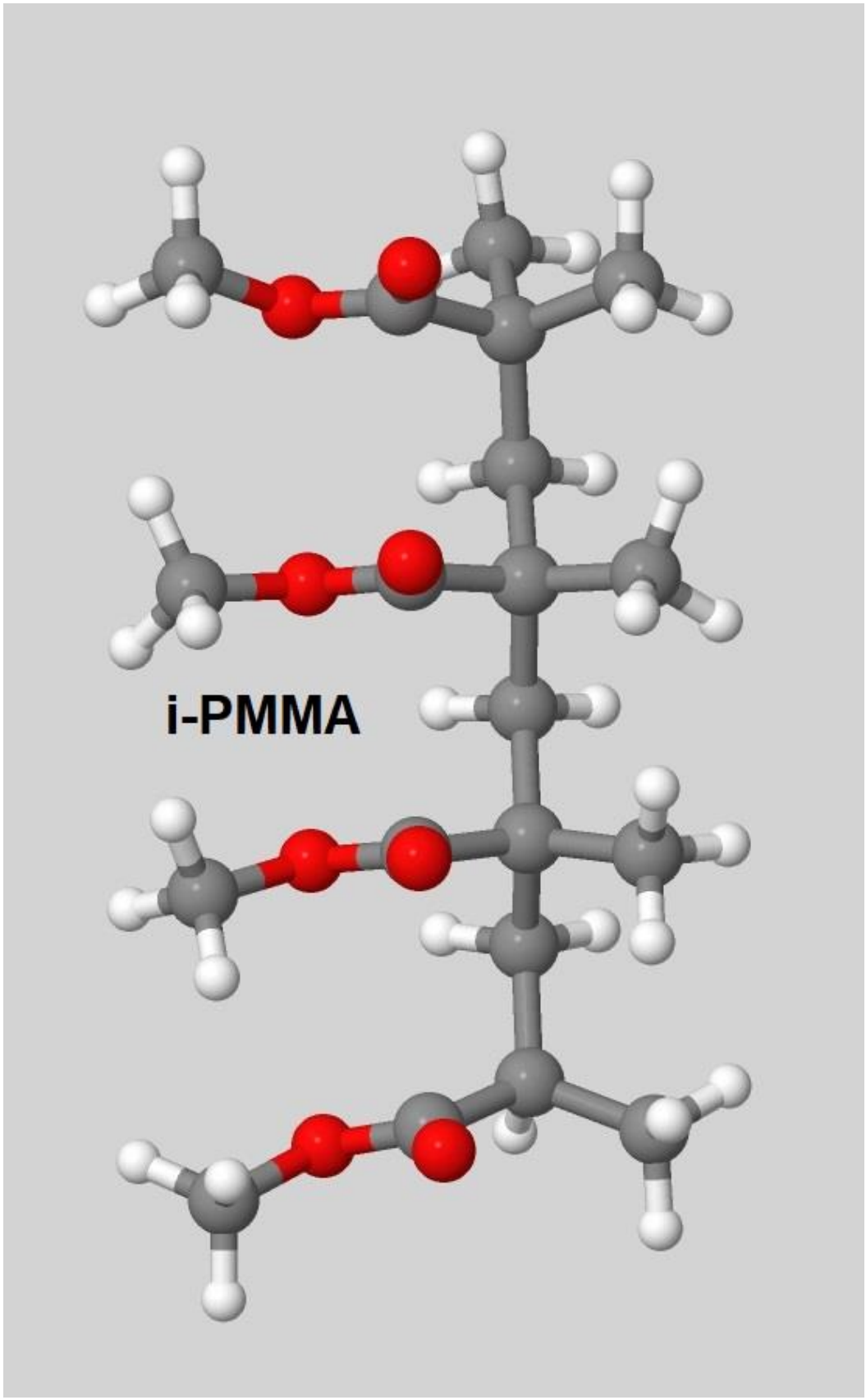

Figure 1a.

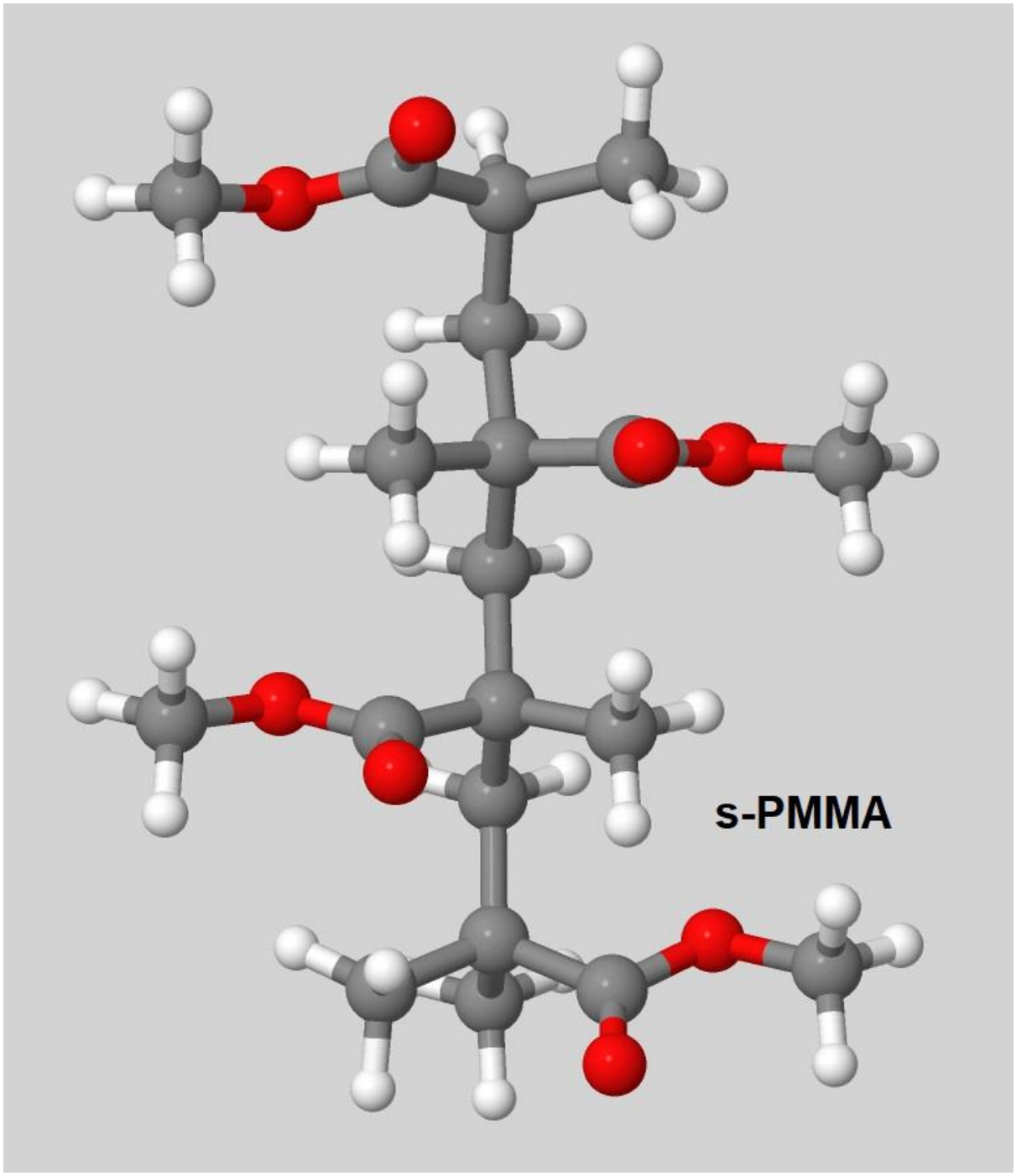

Figure 1b.

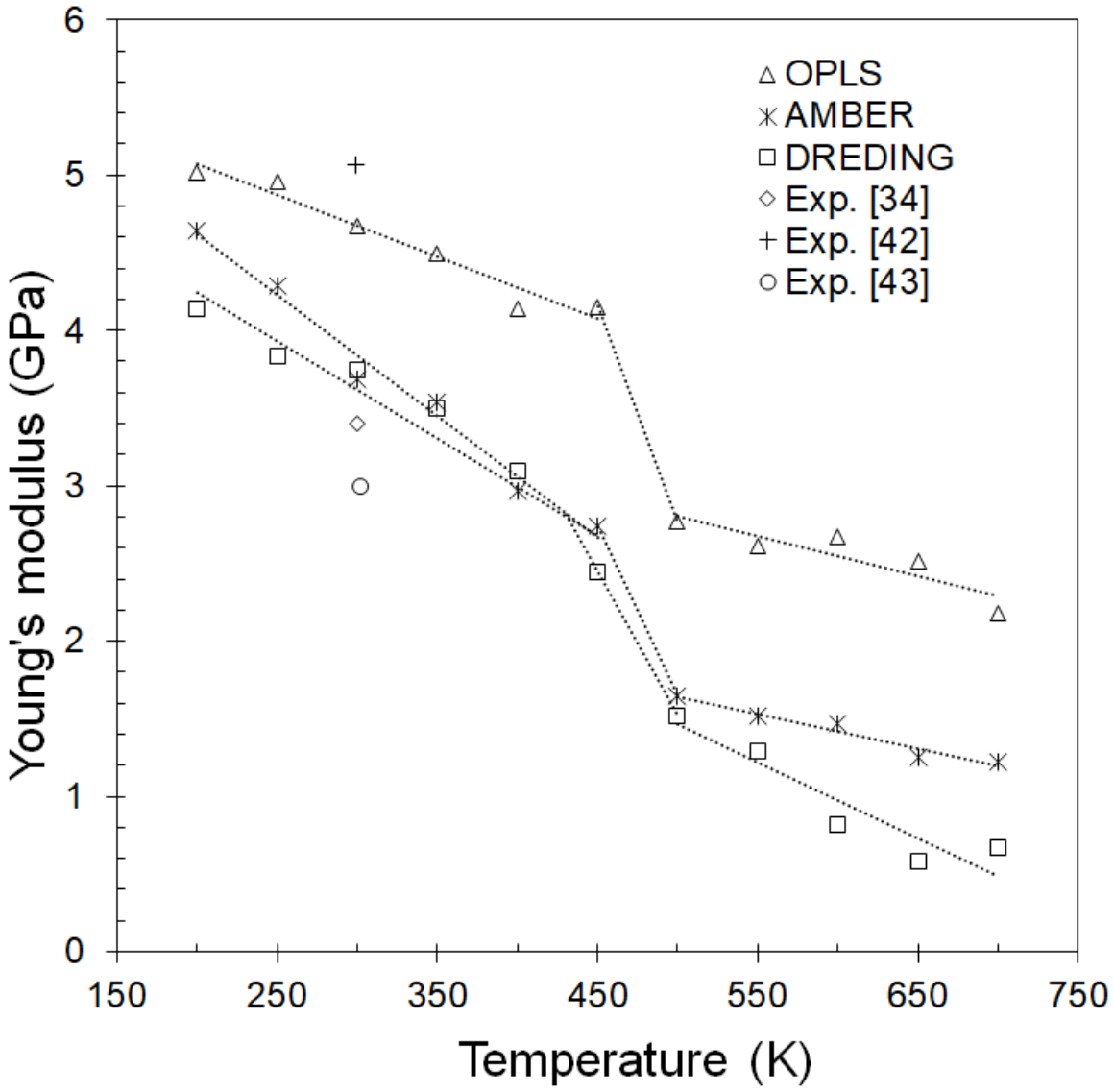
OPLS
AMBER
DREDING
Exp. [34]
Exp. [42]
Exp. [43]
Young's modulus (GPa)
Temperature (K)
0
1
2
3
4
5
6
150
250
350
450
550
650
750

Figure 2

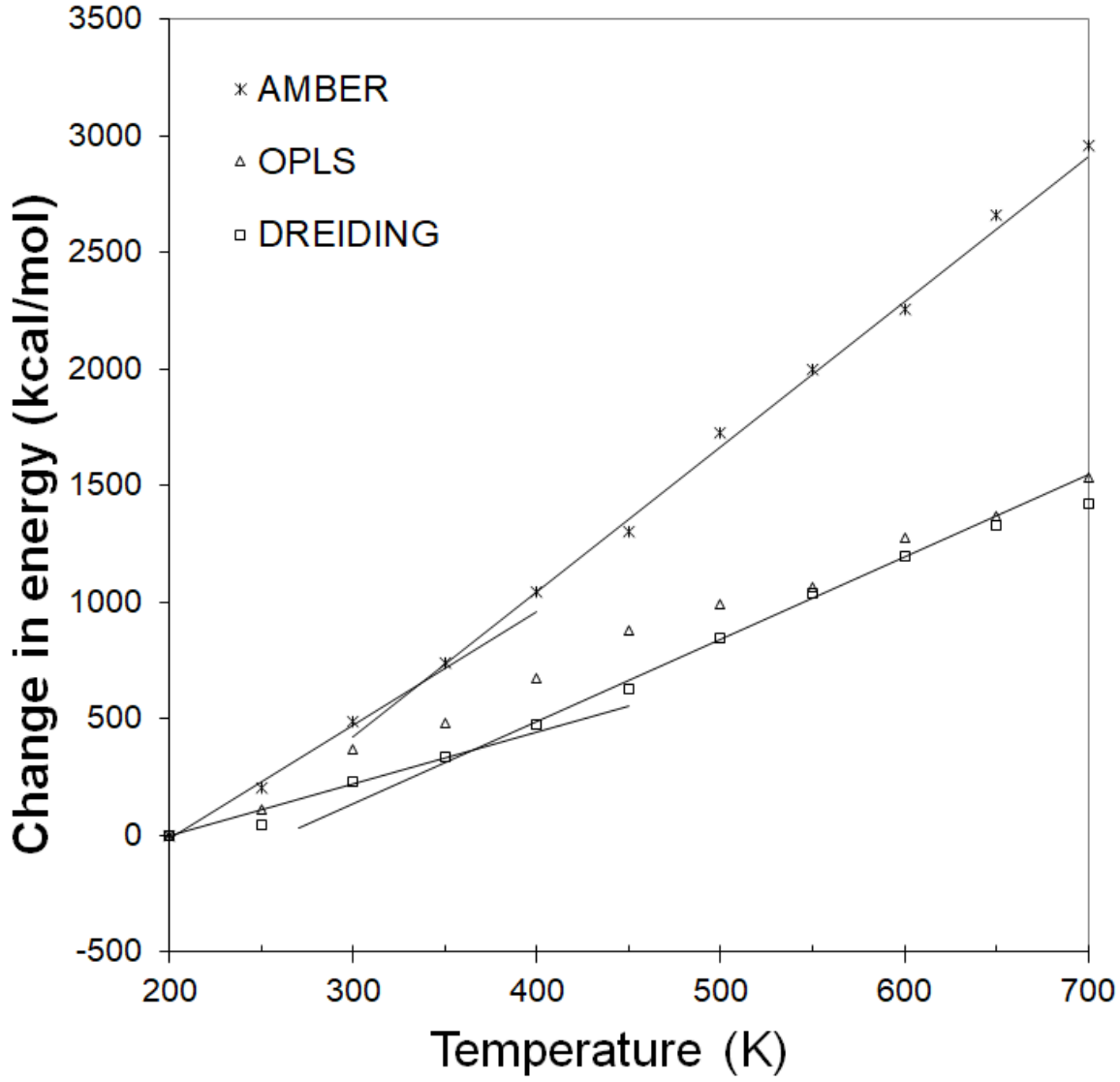
AMBER
OPLS
DREIDING
Change in energy (kcal/mol)
Temperature (K)
3500
3000
2500
2000
1500
1000
500
0
-500
200
300
400
500
600
700

Figure 3

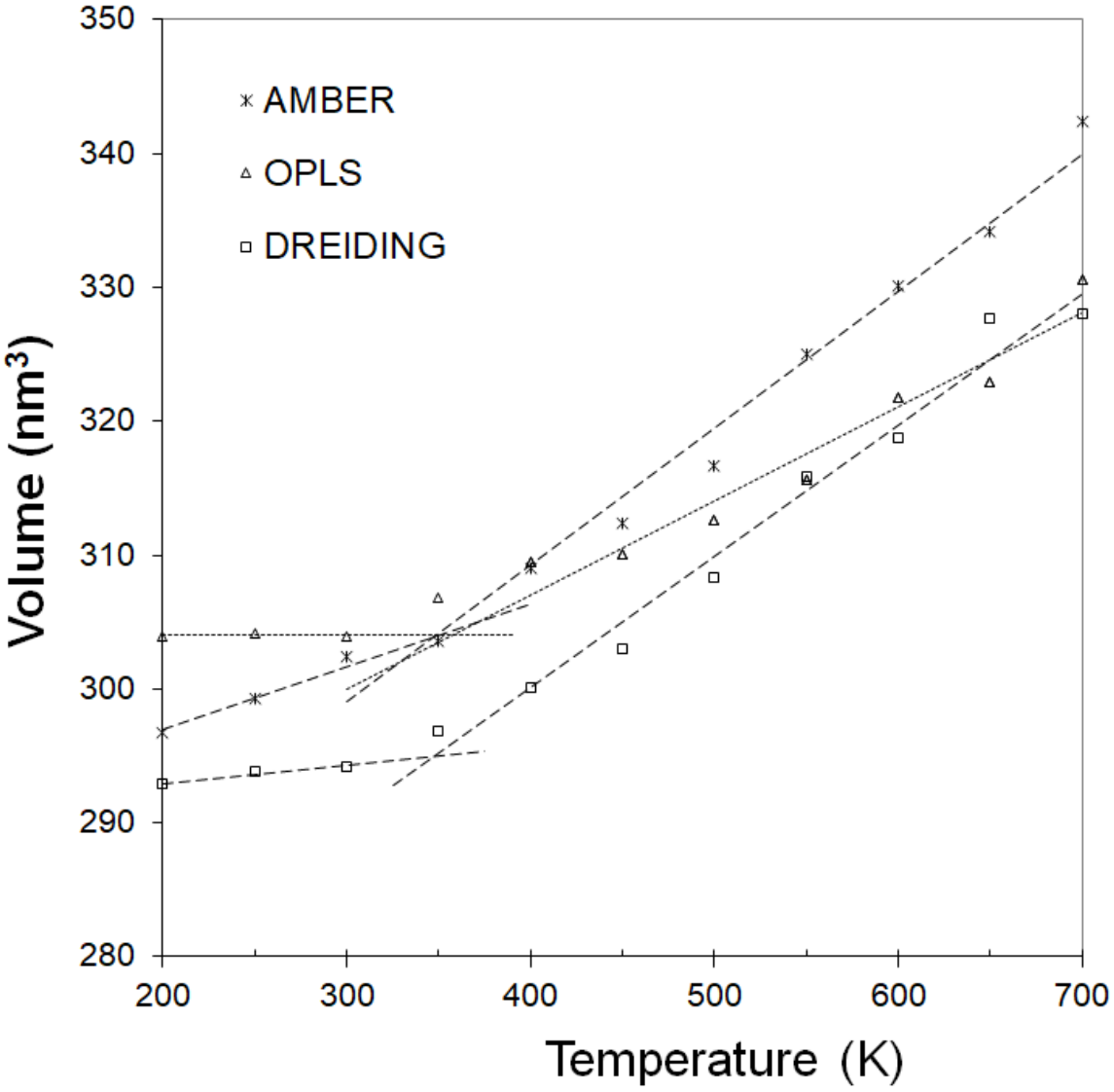
AMBER
OPLS
DREIDING
Volume (nm³)
Temperature (K)
350
340
330
320
310
300
290
280
200
300
400
500
600
700

Figure 4